

Clinical Trial

Discovery of calcite as a new pro-inflammatory calcium-containing crystal in human osteoarthritic synovial fluid



Tom Niessink # † * ¹, Roderick H.M.J. Stassen ‡ ¹, Brenda Kischkel §, Patricia Vuscan §, Peter J. Emans ‡, Guus G.H. van den Akker ‡, Matthijs Janssen #, Leo A.B. Joosten § ¶, Cees Otto †, Tim J.M. Welting ‡, Tim L. Jansen #

Department of Rheumatology, VieCuri Medical Centre, Tegelseweg 210, 5912 BL Venlo, the Netherlands

† Personalized Therapeutics and Diagnostics, Department of Bioengineering Technology, University of Twente, Drienerlolaan 5, 7522 NB Enschede, the Netherlands

‡ Department of Experimental Orthopaedics, Maastricht University Medical Centre, P. Debyelaan 25, 6229 HX Maastricht, the Netherlands

§ Department of Internal Medicine, Radboud University Medical Centre, Geert Grooteplein Zuid 8, 6525 GA Nijmegen, the Netherlands

¶ Department of Medical Genetics, Iuliu Hatieganu University of Medicine and Pharmacy, Str. Pasteur, Nr. 6, 400012 Cluj-Napoca, Romania

ARTICLE INFO

Article history:

Received 11 January 2024

Accepted 21 May 2024

Keywords:

Calcium crystals

Raman spectroscopy

Biomarkers in osteoarthritis

Crystal induced inflammation

SUMMARY

Objective: We aimed to characterize calcium-containing crystals present in synovial fluid from patients with knee osteoarthritis (OA) using Raman spectroscopy, and specifically investigate the biological effects of calcite crystals.

Design: Thirty-two synovial fluid samples were collected pre-operatively from knee OA patients undergoing total joint arthroplasty. An integrated Raman polarized light microscope was used for identification of crystals in synovial fluid. Human peripheral blood mononuclear cells (PBMC's), human OA articular chondrocytes (HACs) and fibroblast-like synoviocytes (FLSs) were exposed to calcite crystals. Expression of relevant cytokines and inflammatory genes were measured using enzyme-linked immuno sorbent assay (ELISA) and real-time polymerase chain reaction (PCR).

Results: Various calcium-containing crystals were identified, including calcium pyrophosphate (37.5 %) and basic calcium phosphate (21.8 %), but they were never found simultaneously in the same OA synovial fluid sample. For the first time, we discovered the presence of calcite crystals in 93.8 % of the samples, while dolomite was detected in 25 % of the cases. Characterization of the cellular response to calcite crystal exposure revealed increased production of innate immune-derived cytokines by PBMC's, when co-stimulated with lipopolysaccharide (LPS). Additionally, calcite crystal stimulation of HACs and FLSs resulted in enhanced secretion of pro-inflammatory molecules and alterations in the expression of extracellular matrix remodeling enzymes.

Conclusions: This study highlights the unique role of Raman spectroscopy in OA crystal research and identified calcite as a novel pro-inflammatory crystal type in OA synovial fluid. Understanding the role of specific crystal species in the OA joint may open new avenues for pharmacological interventions and personalized approaches to treating OA.

© 2024 The Author(s). Published by Elsevier Ltd on behalf of Osteoarthritis Research Society International.

This is an open access article under the CC BY license (<http://creativecommons.org/licenses/by/4.0/>).

Introduction

The ubiquitous presence of calcium-containing crystals in osteoarthritis (OA) pathology is of significant interest.¹ Crystals may cause inflammation through the innate immune system, with detrimental effects.¹ Expanding our knowledge on the different types of

calcium-containing crystals in OA can potentially uncover novel therapeutic avenues in OA.^{1,2}

Detection of calcium-containing crystals is challenging with conventional methods like polarized light microscopy (PLM).^{3–5} Spectroscopic methods such as Raman spectroscopy, Fourier-Transform Infrared spectroscopy (FTIR) and energy dispersive X-ray (EDX) can identify pathognomonic calcium crystals. Raman spectroscopy is a non-destructive laser-based form of vibrational spectroscopy and has been applied to identify calcium pyrophosphate (CPP) in synovial fluid^{6,7} and calcium crystals in articular tissue.⁸ FTIR is also a

* Correspondence to: Drienerlolaan 5, 7522 NB Enschede, the Netherlands.

E-mail addresses: t.niessink@utwente.nl, tniessink@viecuri.nl (T. Niessink).

¹ Contributed equally as first authors of this paper.

form of vibrational spectroscopy and has been applied to detect calcium crystals in synovial fluid and articular tissue^{5,9} EDX is based on x-ray diffraction and offers a highly specific characterization method.¹⁰ EDX requires sample preparation, however, limiting its potential clinical use.⁵

Both CPP and basic calcium phosphate (BCP) crystals are associated with OA. CPP presents as rhomboid- or tubulus-shaped crystals with weak positive birefringence in PLM. BCP crystals do not have distinctive birefringent features and are therefore not easily identified with PLM. Imaging can be performed with alizarin red staining or advanced techniques such as scanning electron microscopy.^{11,12} BCP crystals are present in 100 % of articular cartilage specimens derived from end-stage knee OA patients.¹³ In synovial fluids, CPP crystals are found in 23–32 % of all knee OA patients, while BCP crystals were found in 22–49 % of all knee OA patients.^{11,12,14,15} Calcium oxalate is another type of calcium crystal, occasionally found in synovial fluid, although it is not associated with OA.¹⁶ Calcium oxalate can consist in two forms: monohydrate (COM) and dihydrate (COD). COM presents as irregular squares or rod-like crystals, while COD presents with a distinctive envelope shape; both are positively birefringent with PLM.¹⁶

The deposition of BCP and CPP crystals can alter tissue biomechanics due to degenerative changes in the affected joint.¹⁷ Both crystal species are considered Damage-Associated Molecular Patterns (DAMPs), since they can interact with fibroblasts, chondrocytes, and macrophages.¹⁸ Cellular recognition of BCP and CPP crystals can activate several signaling pathways, resulting in the production of metalloproteinases, pro-inflammatory cytokines (TNF, IL-6, and IL-1 β), nitric oxide, and induces apoptosis of articular chondrocytes and synovial fibroblasts.^{19,20} Innate and adaptive immune cells can infiltrate the joint tissue and play a significant role in the pathogenesis of OA. The presence of these mononuclear cells in human peripheral blood (PBMCs), made this a common model to study the effects of crystals on the immune system.²¹ Activation of pro-inflammatory gene expression in response to calcium-containing crystals has also been observed in non-immune-related cell types in the synovial joint. Stimulation of fibroblast-like synoviocytes (FLS) with BCP crystals increased production of prostaglandin E2 (PGE₂).²² In addition, stimulation of OA FLS with BCP crystals increased expression of *MMP-1*,²³ which was shown to be RAS/MAPK signaling dependent.²⁴ Stimulation of OA human articular chondrocytes (OA HACs) with BCP crystals increased expression of IL-6, MMP-1 and MMP-13, while decreasing *COL2A1* and *ACAN*.²⁵ Together, these events contribute to OA.^{19,20}

Calcium carbonate crystals were found as a potential fourth type of calcium crystal in OA cartilage with Raman spectroscopy.⁸ These have been demonstrated to play a role in cartilage hypomineralization in advanced OA.²⁶ In synovial fluids, calcium carbonates have been identified with EDX. Swan et al. identified calcium carbonate in a patient with OA¹⁰ and Li et al. identified calcium carbonate in several unselected synovial fluid samples.²⁷ Furthermore, Reginato et al. identified several cases of body-foreign synovitis attributed to calcium carbonate present in the synovial space due to penetration by sea urchin spines.²⁸

In this work, we utilized an integrated approach of PLM and Raman spectroscopy. In a previous study, we have demonstrated the ability to identify a range of calcium containing crystals with this method, including calcium carbonate which was present in 32 % of unselected synovial fluid samples.²⁹ In the present work, we performed three experiments. We first analyzed thirty-two synovial fluids from patients with end-stage OA with Raman spectroscopy to determine the prevalence of the different types of calcium-

containing crystals in these samples. We identified a high prevalence of calcite crystals, a calcium carbonate polymorph. To determine whether these have a meaningful role in OA, we investigated the pro-inflammatory and pro-degenerative properties of this novel synovial fluid crystal species on OA HACs, OA FLS (both from different donors) and investigated the pro-inflammatory properties of calcite on PBMCs.

Methods

Synovial fluid analysis

Synovial fluid samples from 31 OA patients were derived from the Maastricht University Medical Centre (MUMC+) experimental orthopedics joint collection study (METC permit 2017–0183). Samples were drawn during the arthroplasty procedure, after the administration of anesthesia and before opening the knee. The population includes adult males and females. Samples were frozen at -80°C and stored for several months in plastic Eppendorf tubes (Eppendorf, Nijmegen, the Netherlands) without preservatives. Relevant patient data was retrieved retrospectively from electronic health records. Patients gave written informed consent before collection and use of their synovial fluid and data. From each patient, the most recent available knee X-ray was analyzed for Kellgren-Lawrence grading (0–4) and chondrocalcinosis (meniscal, hyaline cartilage, tendons, and synovial capsule was assessed separately) by an experienced orthopedic surgeon.

Samples were analyzed with an iRPolM integrated Raman polarized light microscope (Hybriscan Technologies B.V., Nijkerk, the Netherlands). For each sample, 20 μL of synovial fluid was pipetted on a microscope slide (Menzel glazer, Thermo Fisher, Waltham, MA, USA). A trained analyst (TN) used the integrated polarized light microscope to localize crystals. Crystals were selected based on their morphology, birefringence, and overall appearance. The presence of birefringence was used as an aid for crystal localization but was not a prerequisite for selection. An area of interest around the localized crystals was then selected and scanned with the integrated Raman spectrometer. Calibration and measurement procedures are given in **SI1**. Spectra were analyzed and qualitatively scored by a TN who compared the measurements with a previously established Raman spectral database.²⁹ We counted all crystals with a certain spectrum in every sample. Graphs were made with MATLAB R2023b.

Peripheral blood mononuclear cells (PBMCs) isolation and treatments

Buffy coats were obtained after informed consent from healthy volunteers (Sanquin Bloodbank, Nijmegen, The Netherlands). The study was approved by Ethics Committee of Radboud University Nijmegen (NL32357.091.10) and all the experiments were conducted according to the principle expressed in the Declaration of Helsinki. Isolation of PBMCs was performed by blood dilution in PBS, after which differential density centrifugation was done over Ficoll-Paque (GE Healthcare, Zeist, The Netherlands), as previously described.³⁰ PBMCs were resuspended in Roswell Park Memorial Institute Medium (RPMI) 1640 culture medium (Roswell Park Memorial Institute medium, Invitrogen, USA) supplemented with 10 $\mu\text{g}/\text{mL}$ gentamicin, 10 mM L-glutamine, and 10 mM pyruvate (Gibco, UK). Cell counting was performed using the Sysmex hematology instrument, with the concentration of cells adjusted to $5 \times 10^6/\text{mL}$ (or 5×10^5 cells in 100 $\mu\text{L}/\text{well}$) in round-bottom 96-well plates. Next, cells were stimulated with 10 ng/mL LPS (or 40 ng in 50 $\mu\text{L}/\text{well}$) and/or

25 $\mu\text{g}/\text{mL}$ calcite (or 100 ng in 50 $\mu\text{L}/\text{well}$, SkySpring Nanomaterials Inc., Houston, Texas, USA) and 300 $\mu\text{g}/\text{mL}$ monosodium urate (MSU) (or 1200 μg in 50 $\mu\text{L}/\text{well}$) crystals. The final volume per well was adjusted to 200 μL with RPMI under conditions with a single stimulation followed by incubation at 37 °C, 5 % CO_2 . After 24 h, the supernatants were collected for cytokine measurements by enzyme-linked immuno sorbent assay (ELISA).

Isolation of human OA articular chondrocytes (HACs) and FLSs and treatments

OA HACs and FLS were isolated from surgical waste material retrieved from different patients than the PBMCs and synovial fluids (METC-2017–0183). Chondrocytes were isolated as previously described.³¹ In short, cartilage was digested in type II collagenase solution overnight (37 °C). The obtained cell suspension was passed through a 70 μm cell strainer. Isolated chondrocytes were cultured in DMEM/F12 supplemented with 10 % fetal calf serum, 1 % antibiotic/antimycotic (Gibco, Fisher scientific, New Hampshire, USA) and 1 % non-essential amino acids (Gibco, Fisher scientific, New Hampshire, USA). Since isolated chondrocytes lose their phenotype and become fibroblastic after multiple passages, we explicitly cultured chondrocytes only 1 passage and used them for our experiments. Human OA FLSs were isolated in a similar manner. Fat tissue was separated from the synovium and dissected further. These dissected tissue sections were placed in type II collagenase solution overnight at 37 °C. After digestion, cells were isolated using a 70 μm cell strainer and cultured in DMEM/F12 supplemented with 10 % fetal calf serum, 1 % antibiotic/antimycotic (Gibco, Fisher scientific, New Hampshire, USA) and 1 % non-essential amino acids (Gibco, Fisher scientific, New Hampshire, USA) until passage 1. Both cell types were seeded at a density of 30.000 cells/ cm^2 . Both cell types were exposed to 50 $\mu\text{g}/\text{mL}$ calcite crystals for a period of 48 h at 37 °C and 5 % CO_2 .

Cytotoxicity assay in PBMCs

Lactate dehydrogenase (LDH) release was measured in cell culture supernatants using the CytoTox 96 nonradioactive cytotoxicity assay (Promega, WI, USA) according to manufacturer's instructions. Briefly, PBMCs were pre-incubated for 1 h with 10 ng/mL of polymyxin B (Bedford Laboratories, Bedford, OH) before stimulation with the concentrations of 1, 10, 25, and 50 $\mu\text{g}/\text{mL}$ of calcite crystals. After 24 h of incubation, secreted LDH was measured in the cell culture supernatants. The final values are expressed as a percentage of dead cells.

Cytokine measurements

Production of IL-1 β , IL-1Ra, IL-6, CXCL8 and TNF was measured using commercial ELISA kits following the manufacturer's protocol (R&D Systems, Minneapolis, USA). PGE₂ levels were determined with ELISA (Cayman Chemical, Ann Arbor, USA) according to manufacturer's protocol.

RNA isolation and quantification by real-time PCR (RT-qPCR)

Total ribonucleic acid (RNA) extraction of PBMCs was done with the NucleoSpin mini kit for RNA purification (Macherey-Nagel, Düren, Germany) according to manufacturer's instructions. RNA from OA HACs and FLS was isolated by the TRIzol™ method as previously described.²⁵ For all samples, quantification of the isolated

RNA was done using the Nanodrop 2000 UV-visible spectrophotometer (Thermo Fisher Scientific, Massachusetts, USA). Synthesis of cDNA from 200 ng RNA was done using the iScript™ Reverse Transcriptase (Invitrogen, Massachusetts, USA) or Random hexamer synthesis method (Promega, WI, USA). Relative gene expression was determined using the SYBR Green Real-time polymerase chain reaction (PCR) Assay (Applied Biosystems, Foster City, CA, USA) on PBMCs using an Applied Biosystems StepOne PLUS qPCR machine, while for OA HACs and FLS a Bio-rad CFX96 Touch Real-Time PCR machine was used. *PPIA* and *RPL37A* were used as reference gene, for calculating relative expression following the $\Delta\Delta\text{Ct}$ method. Primer sequences are reported in Table S1.

Statistical testing

The interrater reliability in identifying the presence of knee chondrocalcinosis between radiography and Raman spectroscopy was calculated with absolute agreement. For the bioassay experiments, data are given as mean \pm standard error of the mean (SEM). Normality of the data was tested with use of the D'Agostina & Pearson test. In case of normal distribution, a paired or unpaired Students' T-test was performed, otherwise data was analyzed using a Wilcoxon matched-pairs signed-rank test as indicated in the figure legends. P-values of * $p < 0.05$, were considered statistically significant. In any case, we used all available samples for the experiments, to reach a highest-as-possible significance.

Results

Calcium-containing crystals were present in all (100 %) of the 32 samples (Table 1). Thirty-one (93.8 %) samples contained calcite crystals. Dolomite crystals were present in eight (25.0 %) samples, seven (21.9 %) samples contained both types of carbonate crystals. CPP crystals were present in twelve (37.5 %) samples. BCP crystals were present in seven (21.8 %) samples. Calcium oxalate crystals were present in eight (22.8 %) samples, three of which were identified as dihydratic and five of which were identified as monohydratic. When calcium oxalate was detected it was in very low amounts (1–2 crystals per 20 μL sample). Most of the samples (78.1 %) contained more than one type of calcium crystal, but none of the samples contained both CPP and BCP. MSU crystals were found in one patient, who had a known diagnosis of gout. There was a 68.8 % agreement between radiographic chondrocalcinosis and Raman spectroscopic identification of CPP. Crystals COD, COM, CPP, BCP and MSU were only identified in patients > 60 years of age, calcite, and dolomite could also be found in younger patients.

Calcium-containing crystals were identified by their distinct Raman spectra (Fig. 1). We identified hydroxyapatite with a characteristic peak at 960 cm^{-1} . A small peak at 1080 cm^{-1} demonstrates the presence of carbonate substitution in the crystals. There are three known variants of CPP, which are amorphous (a-CPP), monoclinic (m-CPP), and triclinic (t-CPP). All identified CPP crystals were of the triclinic variant. tCPP shows characteristic peaks at 150, 355, 540, 756, 1080, 1120, 1182 cm^{-1} and a major peak at 1049 cm^{-1} . We have conducted several experiments to ensure that the identified crystals were not present due to potential experimental artefacts. We investigated the effect of freezing on the samples, by taking calcite negative and calcite positive synovial fluid samples from different patients. We observed no difference in the number of identified calcites between the initial fluid draw (without having been frozen) and after 3 months of freezing at –80 °C. Furthermore,

Patient	Sex M/F	Age Range	OA Grade 0-4	CC?	Gout? Y/N	Calciumcarbonate		CPP t-CPP	BCP CS-HA	CO COD	COM	MSU MSU
						Calcite	Dolomite					
1	F	61-70	4	T,A	N	++						
2	F	61-70	2	N	N	++		++		+		
3	M	71-80	4	N	N	++						
4	F	71-80	4	M,T,C,A	N	++		++				
5	F	71-80	Unknown	N	N	++			+			
6	F	71-80	4	N	N		+					
7	F	81-90	Unknown	N	N	+	+	+				
8	F	61-70	4	M,T	N	++	+	++				
9	F	71-80	3	N	N	++	+	++				
10	F	51-60	3	N	N	+						
11	F	61-70	4	T,C	N	++					+	
12	F	71-80	4	C	N	++	+					
13	F	71-80	2	N	Y	+	+	+				++
14	M	51-60	3	N	N	++	+					
15	M	71-80	4	N	N	+		+			+	
16	F	61-70	4	N	N						+	
17	F	61-70	Unknown	N	N	+			+			
18	M	71-80	3	M,C,T	N	+		+				
19	F	51-60	1	N	N	++						
20	F	71-80	3	N	N	++			+		+	
21	M	61-70	1	N	N	++					+	
22	F	51-60	3	M,C,A	N	+						
23	M	71-80	3	N	N	++				+		
24	M	61-70	3	N	N	+						
25	F	71-80	4	N	N	++	+		+	+		
26	M	71-80	4	N	N	++			+			
27	M	71-80	4	M,A	Y	++		++				
28	M	61-70	4	N	Y	+			+			
29	F	81-90	4	N	N	++		+				
30	F	71-80	4	N	N	++			+			
31 L	M	71-80	4	T,A	N	+		+				
32 R	M	71-80	4	A	N	++		++				

Table 1

Overview of relevant patient data and results of Raman spectroscopic analysis. Patient data retrieved in retrospective analysis, crystals were identified with a Hybriscan H-iRPolM Raman Spectrometer. OA grade was determined on the Kellgren-Lawrence grading system. Chondrocalcinosis was determined with the most recently available knee X-ray. CC = Chondrocalcinosis (M = meniscal, C = hyaline cartilage, T = tendons, A = articular capsule), CPP = calcium pyrophosphate, tCPP = triclinic calcium pyrophosphate, BCP = Basic calcium phosphate, CS-HA = calcium substituted hydroxyapatite, CO = calcium oxalate, COD = calcium oxalate dihydrate, COM = calcium oxalate monohydrate, MSU = monosodium urate. A score of + was given to samples with 1–2 identified crystals and a score of ++ was given to samples with 3 crystals per 20 μ L of synovial fluid.

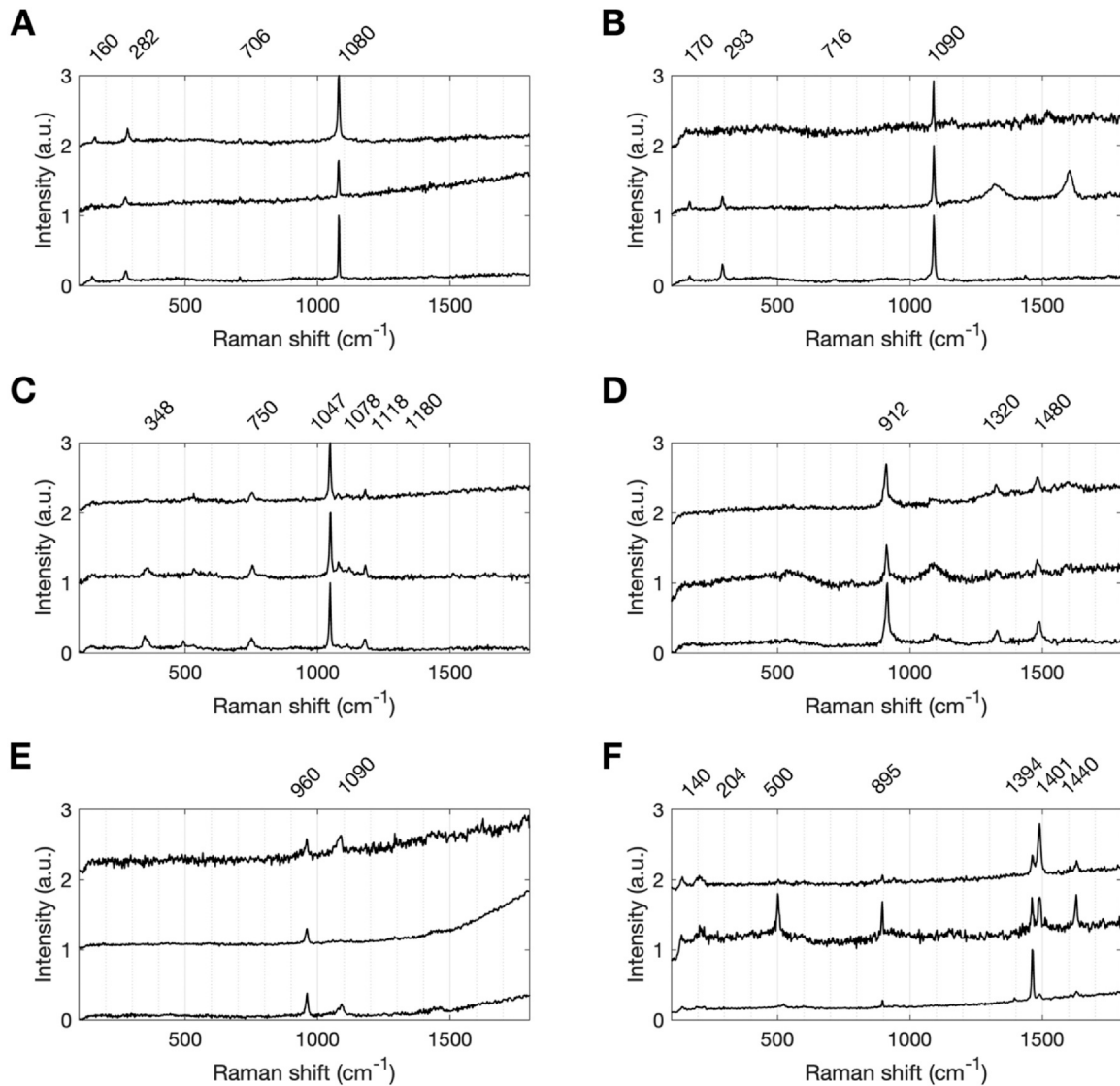


Fig. 1

Compilation of Raman spectra from calcium containing crystals identified in synovial fluid samples of patients clinically diagnosed with OA, together with characteristic peak locations. A) Calcite. B) Dolomite. C) triclinic CPP. D) Calcium oxalate dihydrate. E) Hydroxyapatite, visual with and without 1090 carbonate substitution peak. F) Calcium oxalate monohydrate. Spectra were measured with the iRPolM integrated Raman spectrometer, with a 1 s/spectrum integration time and a 10 mW under-the-objective laser power. Spectra are normalized. All displayed spectra are from different patients within the cohort.

empty microscope slides without synovial fluid were scrutinized on the presence of calcite crystals present there. No crystals were found.

To investigate whether calcite crystals evoke a pathological response in cell types relevant to the OA joint, we evaluated the catabolic capacity of calcite crystals on OA FLS isolated from other donors as used for the synovial fluid analysis. FLS were exposed to 50 $\mu\text{g}/\text{mL}$ calcite crystals (BCP crystals were taken along as a pro-inflammatory reference stimulus relevant to OA²⁵). Calcite crystals did not affect gene expression levels of *IL-6*, *CXCL8* and *COX-2* (Fig. 2A). In contrast, FLS exposed to calcite crystals increased secretion of *CXCL8* and *PGE₂*, while *IL-6* showed a trend towards increased secretion. Secretion of *TNF* by FLS was not detectable (Fig. 2B).

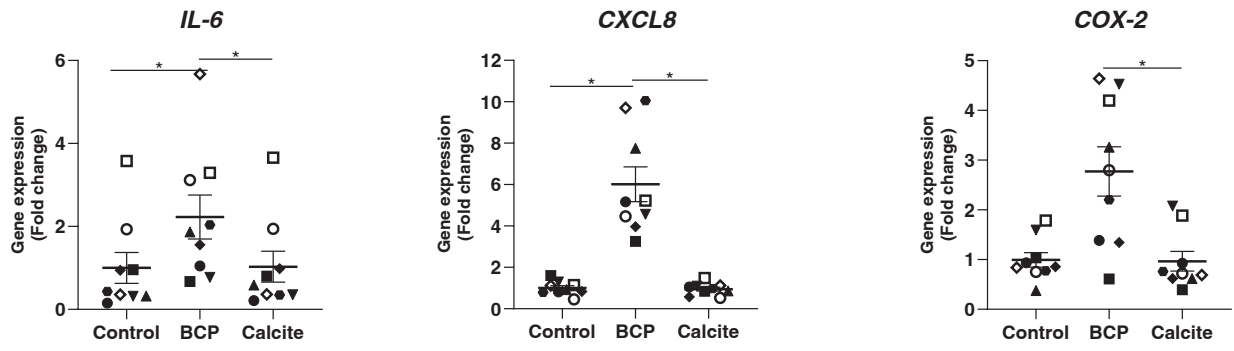
Since OA is characterized by an imbalance in joint tissue matrix homeostasis, we investigated expression of synovial extracellular

matrix components (ECM) and matrix-degrading enzymes by FLS. Calcite crystal exposure of FLS resulted in decreased expression of *COL1A1* and *FN1* (Fig. 2C). No alterations of extracellular matrix degrading enzymes *MMP-1*, *MMP-3* and *ADMTS5* were found in response to calcite crystal exposure (Fig. 2D).

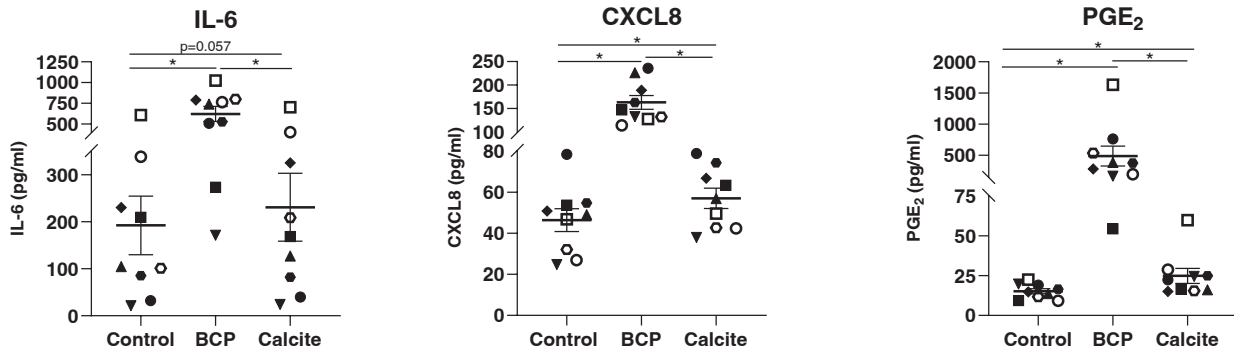
Overall, a specific pro-inflammatory effect of calcite crystals on FLS was observed, which was accompanied by decreased expression of ECM components.

The majority of calcium-containing crystals can be found in the articular cartilage at end-stage OA.¹ Therefore, the effect of calcite crystals was investigated on OA HACs originating from different donors as compared to the synovial fluids in this study. BCP crystals were taken along as pro-inflammatory reference crystals.²⁵ A significant increase in gene expression levels of *IL-6*, *CXCL8*, and *COX-2*

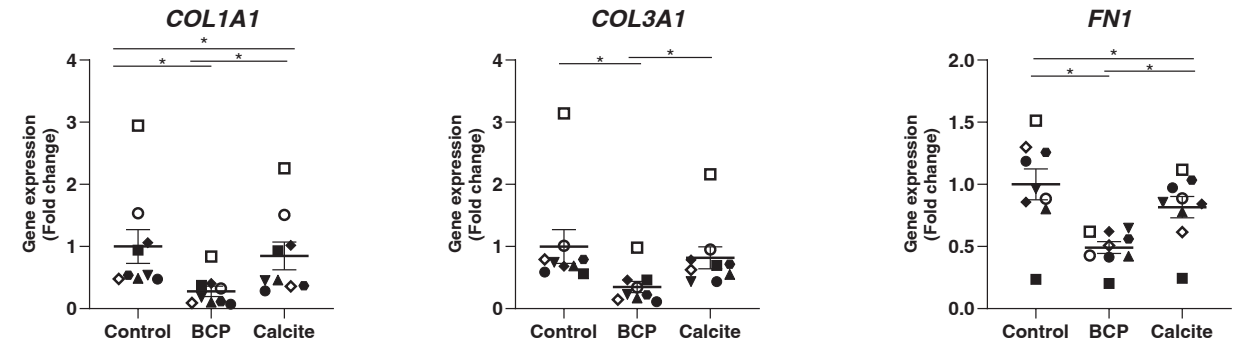
A



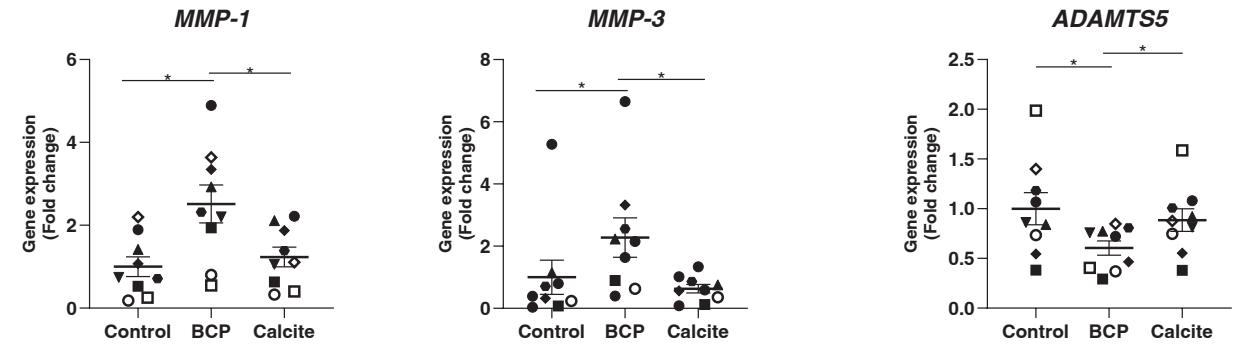
B



C



D



(caption on next page)

Fig. 2

Osteoarthritis and Cartilage

Calcite crystals induce pro-inflammatory molecule secretion in human OA FLSs. A) Nine individual donors of OA FLS were stimulated with either 50 µg/mL BCP crystals or calcite crystals for 48 h. Gene expression analysis of pro-inflammatory molecules IL-6, CXCL8, and COX-2 was determined (n = 3 for each donor). B) Protein secretion of IL-6, CXCL8 and PGE₂ determined with ELISA after 48 h BCP or calcite exposure of 9 individual donors (n = 3 for each donor). C) Gene expression levels of synovial ECM components COL1A1, COL3A1 and FN1 were determined after 48 h in the individual donors (n = 3 for each donor). D) Gene expression levels of matrix degrading enzymes MMP-1, MMP-3 and ADAMTS5 were determined after 48 h BCP or calcite stimulation for all nine individual donors (n = 3 for each donor). In all panels, individual donors are matched with their corresponding symbols. Data are presented as Mean ± SEM. Statistical significance was determined with use of Student's paired T-test in case of normal distribution or Wilcoxon matched-pairs signed rank test. * P.value < 0.05.

was found in response to calcite crystal exposure comparable to BCP crystals (Fig. 3A). These findings were further corroborated by the corresponding secreted protein concentrations in the culture medium after 48 h of exposure (Fig. 3B). OA HACs did not produce *TNF* when exposed to calcite crystals (data not shown). Next, we interrogated whether expression of key cartilage ECM components was affected. Decreased expression of *COL2A1*, *ACAN* and *COL1A1* was observed in response to calcite crystals (Fig. 3C). Besides the decreased expression of these cartilage ECM components, an increase in *MMP-1*, *MMP-3*, and *MMP-13* mRNA was observed (Fig. 3D).

Together, exposure of OA HACs to calcite crystals resulted in increased expression and secretion of pro-inflammatory mediators. From a cartilage homeostasis perspective, calcite crystals drove a decreased expression of key cartilage ECM components and increased expression of specific ECM degrading enzymes.

Next, we investigated the potential inflammatory properties of calcite crystals on immune cells present in isolated human PBMCs. First, we determined the optimal concentration of calcite crystals to stimulate PBMCs. An LDH assay revealed an increase of cytotoxicity by calcite crystals at a highest concentration of 50 µg/mL (Fig. S3A). In the following experiment, we demonstrated that the calcite preparation was free of residual lipopolysaccharide (LPS), since the pre-incubation of PBMCs with or without polymyxin B did not interfere in the production of IL-1β, TNF and IL-1Ra (Fig. S3C). Exposure of PBMCs to calcite led to a dose-dependent increase of IL-1Ra secretion after 24 h of stimulation (Fig. S3B). In contrast, there was no detectable effect of the calcite crystal concentrations on the secretion of the pro-inflammatory cytokines IL-1β, IL-6, or TNF by PBMCs (Fig. S3B).

The poor induction of pro-inflammatory cytokines by crystals themselves, like MSU, BCP and CPPD has previously been reported.³² Co-stimulation is required to induce a pro-inflammatory response.³³ Therefore, we stimulated PBMCs from healthy donors with MSU or calcite crystals with or without the addition of LPS to the media. No significant increase in IL-1β, TNF, and IL-6 production was observed in PBMCs stimulated only with MSU and calcite. Interestingly, IL-1Ra production was significantly increased in cells stimulated with calcite, as opposed to MSU crystals (Fig. 4A). Importantly, the combination of calcite crystals with LPS exposure led to an increase in the cytokine production, which was significantly higher than the LPS-only condition for IL-1β, IL-1Ra, TNF and IL-6 (Fig. 4A).

Additionally, we studied the influence of calcite exposure on *IL1B* and *IL1RN* (IL-1Ra) gene expression in PBMCs. In the first 2 h after calcite exposure, we observed a significant increase of *IL1B*, compared to *IL1RN* (Fig. 4B). However, after 18 h, it was found that calcite crystal exposure of PBMCs led to a significant upregulation of the

IL1RN gene, while *IL1B* expression was decreased in comparison to the initial 2 h time point (Fig. 4B).

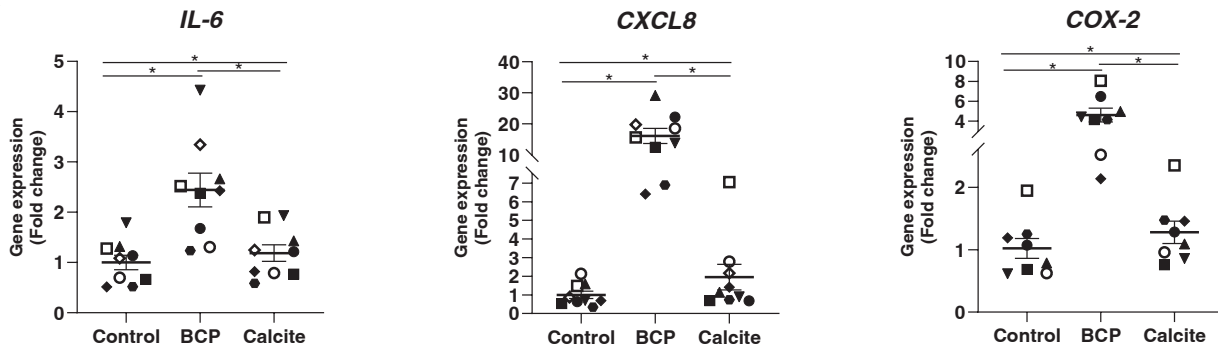
Discussion

In this study, we identified a range of calcium-containing crystals in knee OA synovial fluid with Raman spectroscopy. Calcite was present in almost all (93.8%) samples. Recently, Sorrentino et al. hypothesized a role of calcite as a precursor in BCP biomineralization,³⁴ and calcium carbonate was found in OA cartilage tissue.⁸ Since these are recent observations, data on the biomolecular consequences of calcite crystals for joint-relevant cell behavior is lacking. In our in vitro studies, we unveiled the catabolic effect of calcite crystals on three different primary human cell types present in the OA joint. Data collectively demonstrate that calcite crystals provoke inflammatory responses in human FLSs, articular chondrocytes, and PBMCs, with additional consequences for FLS and HAC ECM maintenance.

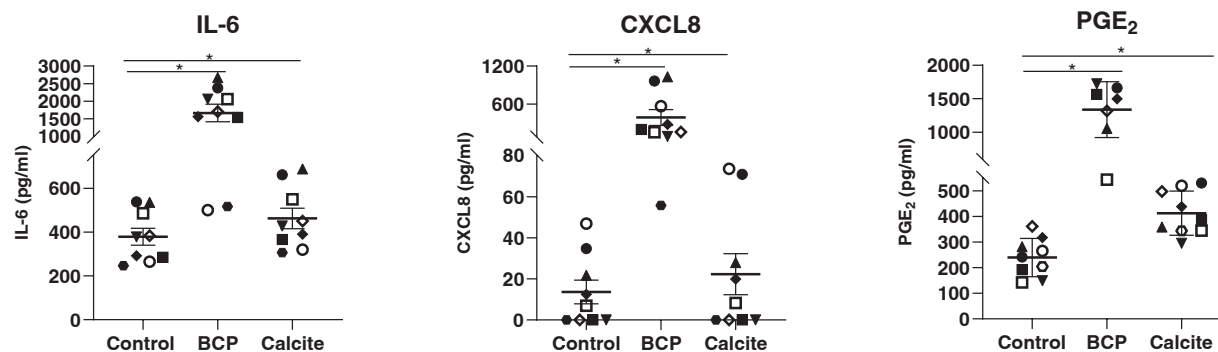
Raman spectroscopic identification of calcium-containing crystals in osteoarthritic synovial fluid allowed for identification of CPP and BCP crystals with a similar sensitivity as scanning electron microscopy¹¹ and PLM.¹² Previous studies with alizarin red and ¹⁴C EHDP (ethane-1-hydroxy 1,1-diphosphonate) binding assay demonstrated higher sensitivity for BCP, and also demonstrated co-occurrence with CPP, which was not demonstrated here with Raman spectroscopy.^{14,15} PLM suffers from bad interrater reliability and bias, especially regarding CPP.³ Raman spectroscopy, however, is more objective than PLM and has near-perfect specificity.³⁵ The dependency on polarized light microscopic crystal localization might influence the sensitivity of our method to the often small and non-birefringent BCP crystals. While scanning electron microscopy is a very sensitive technique, it is often too laborious for clinical practice. Raman spectroscopy can be applied directly and rapidly on fresh synovial fluid samples. Furthermore, Raman spectroscopic analysis of synovial fluid samples allows for extensive chemical characterization of crystals, potentially resulting in new discoveries.

The limitations of this clinical study include a relatively modest sample size (n = 32) and a selection bias of end-stage OA. A side-by-side comparison with matched healthy controls could further establish the specificity of calcite as a biomarker for OA. Raman spectroscopy was chosen to identify crystals. This is a novel method in OA research which limits comparison to previous research. Especially our finding of calcium oxalate crystals, although low in number, is very surprising as these are rarely detected in OA with other modalities. Further studies with alternative, specific, spectroscopic methods such as FTIR or EDX used alongside Raman

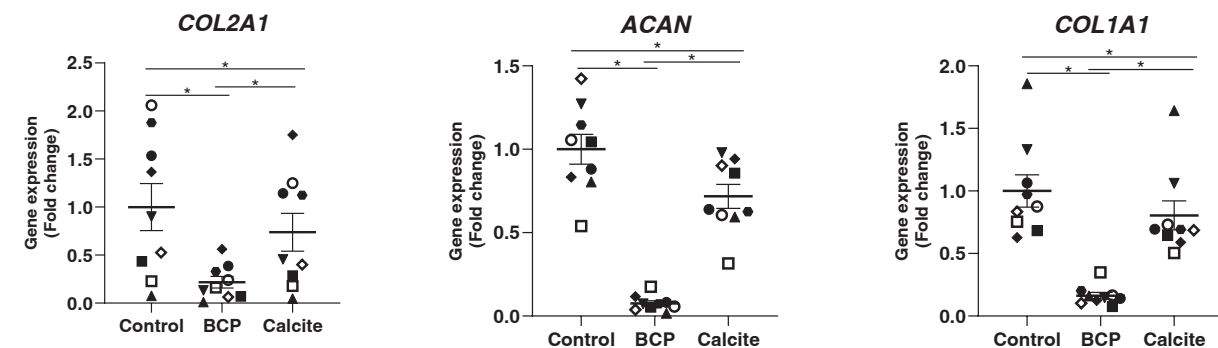
A



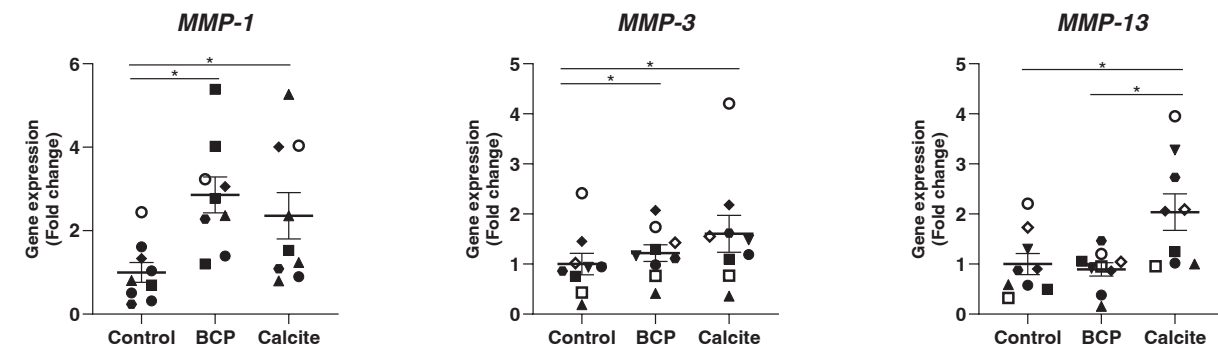
B



C



D



(caption on next page)

Fig. 3

Osteoarthritis and Cartilage

Calcite crystals induce pro-inflammatory molecule secretion and modulate matrix homeostasis in HACs. A) Nine individual donors of OA HACs were stimulated with 50 µg/mL BCP or calcite crystals for 48 h. Gene expression analysis of pro-inflammatory molecules IL-6, CXCL8, and COX-2 was determined (n = 3 for each donor). B) Protein secretion of IL-6, CXCL8 and PGE₂ determined with ELISA after 48 h BCP or calcite exposure of 9 individual donors (n = 3 for each donor). C) Gene expression levels of synovial ECM components COL2A1, ACAN and COL1A1 were determined after 48 h in the individual donors (n = 3 for each donor). D) Gene expression levels of matrix degrading enzymes MMP-1, MMP-3 and MMP-13 were determined after 48 h BCP or calcite stimulation for all nine individual donors (n = 3 for each donor). In all panels, the donors are matched with their corresponding symbol. Data are presented as Mean ± SEM. Statistical significance was determined with use of Student's paired T-test in case of normal distribution or Wilcoxon matched-pairs signed rank test. * P.value < 0.05.

spectroscopy might provide new insights in the prevalence and nature of our novel findings. Previous studies on Raman spectroscopic identification of particles in synovial fluid have successfully used enzymatic digestion to increase crystal yield,²⁷ which might be beneficial for iRPolM analysis.

Stimulation of FLS with calcite crystals resulted in an increased pro-inflammatory response, which was accompanied by changes in expression level of genes involved in extracellular matrix homeostasis, although to a lesser extent as observed with BCP reference crystals. For FLS, calcite crystals induced CXCL8 and PGE₂. Release of pro-inflammatory molecules has been strongly correlated with the presence of synovitis, ultimately resulting in synovial fibrosis.³⁶ In synergy with the pro-inflammatory response, we observed decreased expression levels of *COL1A1* and *FN1* by FLS in response to calcite crystals. More specifically, collagen type I is of key importance for the structure and function of the synovium. This type of collagen is found both in the inner and outer layers. In the outer layer, a dense layer of collagen type I forms the physical membrane.³⁷ In contrast, fibronectin is produced by the synoviocytes residing in the intima.³⁸ Fibronectin expressed by the synoviocytes allows binding of adhesion molecules to their cytoskeleton maintaining the physiological barrier.³⁹ Exposure of FLS to calcite crystals may therefore result in an altered synovial structural integrity, eventually resulting in a decreased barrier function of the synovium as is known for OA.

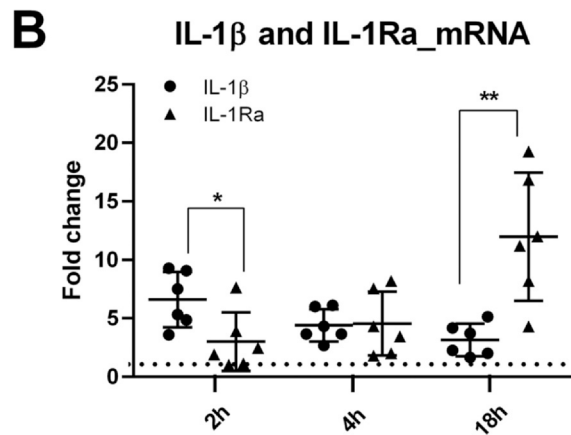
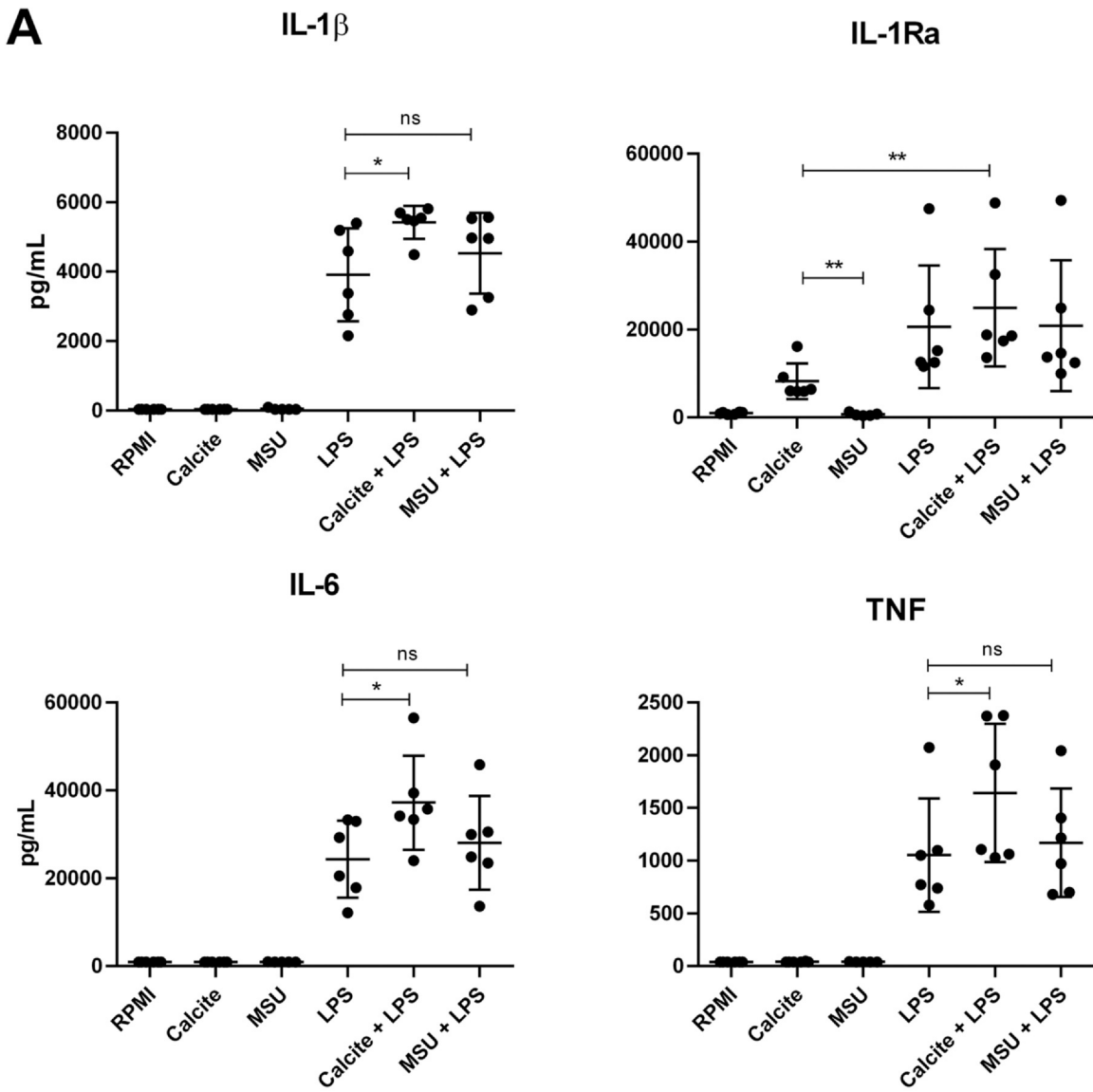
In OA HACs, calcite crystals provoked a mild pro-inflammatory response and altered gene expression of ECM homeostatic genes. However, BCP crystals (taken along as a reference) were more potent in doing so. Interestingly, OA HACs were stimulated to a higher magnitude by calcite as compared to OA FLS. This is evidenced by significantly increased expression of *IL-6*, *CXCL8* and *COX-2* in OA HACs as well as the impact of calcite crystals on genes related to matrix homeostasis in these cells. This difference in responsive magnitude between OA HACs and FLS has also been observed in other studies, with chondrocytes being the most responsive cell type.²³ In OA HACs we observed increased secretion of the pro-inflammatory molecules IL-6 and PGE₂ in response to calcite stimulation. Like BCP crystals, calcite crystal presence may contribute to the pro-inflammatory intra-articular environment as observed in OA pathology.²⁵ In addition to the pro-inflammatory response, we observed a decreased expression in ECM component gene expression. Collagen type II and aggrecan, are main determinants that form the cartilage extracellular matrix.⁴⁰ Alterations in the cartilage ECM resulting from a homeostatic imbalance can lead to articular cartilage degeneration. Decreased expression of key cartilage extracellular

matrix molecules such as collagen type II and aggrecan therefore suggests a catabolic influence of calcite crystals on the homeostasis of chondrocytes, potentially contributing to OA pathology.⁴¹ Furthermore, a calcite-induced increase in extracellular matrix degrading enzyme gene expression was observed. MMP-1, MMP-3 and MMP-13 have been determined as key players in the progression of OA.^{42,43}

PBMCs did not respond in a strong manner to only calcite crystals. However, similar to BCP,³² we observed a synergistic effect of calcite crystals in combination with LPS, that resulted in increased production of IL-1β, TNF and IL-6.^{44,45} Importantly, calcite crystals alone induced an increase of the amount of IL-1β mRNA by PBMCs after 2 h but without significant translation of the IL-1β precursor. In general, the IL-1β precursor requires a stimulus to be induced, in which the first signal ("priming"), drives gene expression and the second signal provides rapid translation of the IL-1β precursor. If a second signal is not provided, the mRNA is degraded.^{46,47} Therefore, our results suggest that calcite crystals alone provide the transcriptional priming signal and LPS the translational signal.

Furthermore, PBMCs stimulated with calcite alone, but not MSU, had increased IL-1Ra production. BCP crystals are also capable of inducing higher concentrations of IL-1Ra compared to MSU.⁴⁸ Initially, the only recognized function of IL-1Ra was as an IL-1 receptor antagonist, competing with IL-1β and IL-1α for binding to the IL-1 receptor. However, it has recently been demonstrated that IL-1Ra also has an intracellular function in promoting autophagy and restore cellular balance.⁴⁹ In OA, the process of autophagy has been shown to be protective for chondrocytes by regulating apoptosis and repairing damaged cell functions. Our results support the role of anti-inflammatory mediators in OA for the resolution of crystal-induced inflammation, since IL-Ra may be being produced by the cells to reduce damage. Together these data provide a cellular basis for calcite crystal contribution to OA pathology across different joint-relevant cell types.

Calcium-containing crystals have previously been described to contribute to the local inflammatory OA environment.² Based on our results calcite can be added as a new species of calcium-containing crystal in OA. Furthermore, we investigated the detrimental effects of these crystals on three different cell types relevant to the OA joint. This further highlights the potential of calcium-containing crystals and their associated inflammatory character as potential targets for intervention.⁵⁰ Subsequent research should focus on investigation of driving factors behind calcite formation to develop therapeutic strategies that potentially modulate the pathobiological course of OA.



(caption on next page)

Fig. 4**Osteoarthritis and Cartilage**

Effect of calcite crystals stimulation on PBMCs. A) Production of IL-1 β , IL-1Ra, IL-6 and TNF was determined with ELISA following 24 h PBMCs stimulation with 25 μ g/mL calcite, 10 ng/mL LPS, 300 μ g/mL MSU and with Calcite or MSU in combination with LPS (n = 6). B) Gene expression levels of IL-1 β and IL-1Ra were determined in 6 individual donors after 2, 4, and 18 h of PBMC stimulation with 25 μ g/mL calcite. Data are presented as Mean \pm SD. Statistical significance was determined with use of Mann-Whitney test or Wilcoxon matched-pairs signed rank test. * P.value < 0.05.

Role of funding source

The funding sources had no role in the inception, execution or reporting of this work.

Declaration of Competing Interest

Cees Otto: Shareholder of Hybriscan Technologies B.V., a company which produces and sells Raman spectrometer devices, including H-iRPolM which was used for this study. Matthijs Janssen, Tim L Jansen: Shareholders of Crystalytics B.V., a company interested in development of tools used for clinical identification of synovial crystals. Tim Welting: Shareholder of Chondropeptix, Inventor of: WO2017/178251, WO2017/178253, WO2023/280615. Guus van den Akker: Inventor of WO2023/280615. All other authors have no potential conflicts of interest to declare.

Acknowledgments

Tom Niessink is funded by a PPP Allowance made available by Health-Holland, Top Sector Life Sciences & Health, to Stichting ReumaNederland to stimulate public-private partnerships (TKI Grant NSP20-1-401).

Tim Welting is funded by a grant from Stichting de Weijerhorst (Bewegen zonder Pijn) and a grant from ReumaNederland (LLP14).

We would like to acknowledge Dr. P.Z. Feczko and Dr. T.A.E.J. Boymans, Dr. M Peters, L. Jutten and A. Cremers for collection of synovial fluid and surgical waste material.

Author contributions

All mentioned authors have made substantial contributions to the conception or design of the work; or the acquisition, analysis, or interpretation of data for the work; helped drafting the work or reviewing it critically for important intellectual content; gave final approval of the version to be published; and agreed to be accountable for all aspects of the work in ensuring that questions related to the accuracy or integrity of any part of the work are appropriately investigated and resolved.

First authors TN (t.niessink@utwente.nl and RS (r.stassen@maastrichtuniversity.nl) take responsibility for the integrity of the complete work, from inception to finished manuscript.

Appendix A. Supporting information

Supplementary data associated with this article can be found in the online version at [doi:10.1016/j.joca.2024.05.004](https://doi.org/10.1016/j.joca.2024.05.004).

References

- Rosenthal AK. Crystals, inflammation, and osteoarthritis. *Curr Opin Rheumatol* 2011;23(2):170–3.
- Conway R, McCarthy GM. Calcium-Containing Crystals and Osteoarthritis: an Unhealthy Alliance. *Curr Rheumatol Rep* 2018;20(3):13.
- Berendsen D, Neogi T, Taylor WJ, Dalbeth N, Jansen TL. Crystal identification of synovial fluid aspiration by polarized light microscopy. An online test suggesting that our traditional rheumatologic competence needs renewed attention and training. *Clin Rheumatol* 2017;36(3):641–7.
- Yavorsky A, Hernandez-Santana A, McCarthy G, McMahon G. Detection of calcium phosphate crystals in the joint fluid of patients with osteoarthritis - analytical approaches and challenges. *Analyst* 2008;133(3):302–18.
- Rosenthal AK, Mandel N. Identification of crystals in synovial fluids and joint tissues. *Curr Rheumatol Rep* 2001;3(1):11–6.
- McGill N, Dieppe PA, Bowden M, Gardiner DJ, Hall M. Identification of pathological mineral deposits by Raman microscopy. *Lancet* 1991;337(8733):77–8.
- Cheng X, Haggins DG, York RH, Yeni YN, Akkus O. Analysis of crystals leading to joint arthropathies by Raman spectroscopy: comparison with compensated polarized imaging. *Appl Spectrosc* 2009;63(4):381–6.
- Casal-Beiroa P, Balboa-Barreiro V, Oreiro N, Pérttega-Díaz S, Blanco FJ, Magalhães J. Optical biomarkers for the diagnosis of osteoarthritis through raman spectroscopy: radiological and biochemical validation using ex vivo human cartilage samples. *Diagnostics* 2021;11(3).
- Rosenthal AK, Mattson E, Gohr CM, Hirschmugl CJ. Characterization of articular calcium-containing crystals by synchrotron FTIR. *Osteoarthr Cartil* 2008;16(11):1395–402.
- Swan A, Chapman B, Heap P, Seward H, Dieppe P. Submicroscopic crystals in osteoarthritic synovial fluids. *Ann Rheum Dis* 1994;53(7):467–70.
- Frallonardo P, Ramonda R, Peruzzo L, Scanu A, Galozzi P, Tauro L, et al. Basic calcium phosphate and pyrophosphate crystals in early and late osteoarthritis: relationship with clinical indices and inflammation. *Clin Rheumatol* 2018;37(10):2847–53.
- Oliviero F, Frallonardo P, Peruzzo L, Ramonda R, Sfriso P, Scanu A, et al. Evidence of silicon dioxide crystals in synovial fluid of patients with osteoarthritis. *J Rheumatol* 2008;35(6):1092–5.
- Fuerst M, Bertrand J, Lammers L, Dreier R, Echtermeyer F, Nitschke Y, et al. Calcification of articular cartilage in human osteoarthritis. *Arthritis Rheum* 2009;60(9):2694–703.
- Derfus BA, Kurian JB, Butler JJ, Daft LJ, Carrera GF, Ryan LM, et al. The high prevalence of pathologic calcium crystals in pre-operative knees. *J Rheumatol* 2002;29(3):570–4.
- Nalbant S, Martinez JAM, Kitumnuaypong T, Clayburne G, Sieck M, Schumacher HR. Synovial fluid features and their relations to osteoarthritis severity: new findings from sequential studies. *Osteoarthr Cartil* 2003;11(1):50–4.
- Lorenz EC, Michet CJ, Milliner DS, Lieske JC. Update on oxalate crystal disease. *Curr Rheumatol Rep* 2013;15(7):340.
- Liu YZ, Jackson AP, Cosgrove SD. Contribution of calcium-containing crystals to cartilage degradation and synovial inflammation in osteoarthritis. *Osteoarthr Cartil* 2009;17(10):1333–40.
- Martinon F, Pétrilli V, Mayor A, Tardivel A, Tschopp J. Gout-associated uric acid crystals activate the NALP3 inflammasome. *Nature* 2006;440(7081):237–41.

19. McCarthy GM, Dunne A. Calcium crystal deposition diseases - beyond gout. *Nat Rev Rheumatol* 2018;14(10):592–602.
20. Pazár B, Ea HK, Narayan S, Kolly L, Bagnoud N, Chobaz V, et al. Basic calcium phosphate crystals induce monocyte/macrophage IL-1 β secretion through the NLRP3 inflammasome in vitro. *J Immunol* 2011;186(4):2495–502.
21. Haseeb A, Haqqi TM. Immunopathogenesis of osteoarthritis. *Clin Immunol* 2013;146(3):185–96.
22. Molloy E, Morgan M, Doherty G, McDonnell B, Hilliard M, O'Byrne J, et al. Mechanism of basic calcium phosphate crystal-stimulated cyclo-oxygenase-1 up-regulation in osteoarthritic synovial fibroblasts. *Rheumatology* 2008;47(7):965–71.
23. McCarthy GM, Westfall PR, Masuda I, Christopherson PA, Cheung HS, Mitchell PG. Basic calcium phosphate crystals activate human osteoarthritic synovial fibroblasts and induce matrix metalloproteinase-13 (collagenase-3) in adult porcine articular chondrocytes. *Ann Rheum Dis* 2001;60(4):399–406.
24. Sun Y, Wenger L, Brinckerhoff CE, Misra RR, Cheung HS. Basic calcium phosphate crystals induce matrix metalloproteinase-1 through the ras/mitogen-activated protein kinase/c-Fos/AP-1/metalloproteinase 1 pathway involvement of transcription factor binding sites AP-1 and PEA-3. *J Biol Chem* 2002;277(2):1544–52.
25. Stassen RHMJ, den Akker GGHv, Surtel DAM, Housmans BAC, Cremers A, Caron MMJ, et al. Unravelling the basic calcium phosphate crystal-dependent chondrocyte protein secretome; a role for TGF- β signaling. *Osteoarthr Cartil* 2023.
26. Wang X, Wu Q, Zhang R, Fan Z, Li W, Mao R, et al. Stage-specific and location-specific cartilage calcification in osteoarthritis development. *Ann Rheum Dis* 2022.
27. Li B, Singer N, Rosenthal A, Unal M, Haggins D, Yeni YN, et al. Chemical characterization of Maltese-cross birefringent particles in synovial fluid samples collected from symptomatic joints. *Jt Bone Spine* 2018;85(4):501–3.
28. Reginato AJ, Ferreiro JL, Riester O'Connor C, Barbasan C, Arasa J, Bednar J, et al. Clinical and pathologic studies of twenty-six patients with penetrating foreign body injury to the joints, bursae, and tendon sheaths. *Arthritis Rheum* 1990;33(12):1753–62.
29. Niessink T, Kuipers C, de Jong BZ, Lenferink ATM, Janssen M, Jansen TL, et al. Raman hyperspectral imaging detects novel and combinations of crystals in synovial fluids of patients with a swollen joint. *J Raman Spectrosc* 2023;54(1):47–53.
30. Giamarellos-Bourboulis EJ, Mouktaroudi M, Bodar E, van der Ven J, Kullberg BJ, Netea MG, et al. Crystals of monosodium urate monohydrate enhance lipopolysaccharide-induced release of interleukin 1 beta by mononuclear cells through a caspase 1-mediated process. *Ann Rheum Dis* 2009;68(2):273–8.
31. Caron MMJ, Emans PJ, Cremers A, Surtel DAM, Coolen MME, van Rhijn LW, et al. Hypertrophic differentiation during chondrogenic differentiation of progenitor cells is stimulated by BMP-2 but suppressed by BMP-7. *Osteoarthr Cartil* 2013;21(4):604–13.
32. Klück V, Boahen CK, Kischkel B, Dos Santos JC, Matzaraki V, Boer CG, et al. A functional genomics approach reveals suggestive quantitative trait loci associated with combined TLR4 and BCP crystal-induced inflammation and osteoarthritis. *Osteoarthr Cartil* 2023;31(8):1022–34.
33. Mylona EE, Mouktaroudi M, Crisan TO, Makri S, Pistiki A, Georgitsi M, et al. Enhanced interleukin-1 β production of PBMCs from patients with gout after stimulation with Toll-like receptor-2 ligands and urate crystals. *Arthritis Res Ther* 2012;14(4):R158.
34. Sorrentino A, Malucelli E, Rossi F, Cappadone C, Farruggia G, Moscheni C, et al. Calcite as a precursor of hydroxyapatite in the early biomineralization of differentiating human bone-marrow mesenchymal stem cells. *Int J Mol Sci* 2021;22(9):4939.
35. Niessink T, Giesen T, Efdé M, Comarniceanu A, Janssen M, Otto C, et al. Test characteristics of Raman spectroscopy integrated with polarized light microscopy for the diagnosis of acute gouty arthritis. *Jt Bone Spine* 2023;90(6), 105611.
36. Zhang L, Xing R, Huang Z, Ding L, Zhang L, Li M, et al. Synovial fibrosis involvement in osteoarthritis. *Front Med* 2021;8, 684389.
37. Smith MD. The normal synovium. *Open Rheumatol J* 2011;5:100–6.
38. Mayston V, Mapp PI, Davies PG, Revell PA. Fibronectin in the synovium of chronic inflammatory joint disease. *Rheumatol Int* 1984;4(3):129–33.
39. Wei Q, Zhu X, Wang L, Zhang W, Yang X, Wei W. Extracellular matrix in synovium development, homeostasis and arthritis disease. *Int Immunopharmacol* 2023;121, 110453.
40. Lian C, Wang X, Qiu X, Wu Z, Gao B, Liu L, et al. Collagen type II suppresses articular chondrocyte hypertrophy and osteoarthritis progression by promoting integrin β 1-SMAD1 interaction. *Bone Res* 2019;7(1):8.
41. Zhong L, Huang X, Karperien M, Post JN. Correlation between gene expression and osteoarthritis progression in human. *Int J Mol Sci* 2016;17(7):1126.
42. Vincenti MP, Brinckerhoff CE. Transcriptional regulation of collagenase (MMP-1, MMP-13) genes in arthritis: integration of complex signaling pathways for the recruitment of gene-specific transcription factors. *Arthritis Res Ther* 2002;4:1–8.
43. Leong DJ, Gu XI, Li Y, Lee JY, Laudier DM, Majeska RJ, et al. Matrix metalloproteinase-3 in articular cartilage is upregulated by joint immobilization and suppressed by passive joint motion. *Matrix Biol* 2010;29(5):420–6.
44. Choi MC, Jo J, Park J, Kang HK, Park Y. NF- κ B signaling pathways in osteoarthritic cartilage destruction. *Cells* 2019;8:7.
45. Zhang G, Ghosh S. Toll-like receptor-mediated NF-kappaB activation: a phylogenetically conserved paradigm in innate immunity. *J Clin Invest* 2001;107(1):13–9.
46. Kaspar RL, Gehrke L. Peripheral blood mononuclear cells stimulated with C5a or lipopolysaccharide to synthesize equivalent levels of IL-1 beta mRNA show unequal IL-1 beta protein accumulation but similar polyribosome profiles. *J Immunol* 1994;153(1):277–86.
47. Dinarello CA. How interleukin-1 β induces gouty arthritis. *Arthritis Rheum* 2010;62(11):3140–4.
48. Scanu A, Oliviero F, Luisetto R, Ramonda R, Doria A, Punzi L, et al. Effect of pathogenic crystals on the production of pro- and anti-inflammatory cytokines by different leukocyte populations. *Immunobiology* 2021;226(1), 152042.
49. van de Veerdonk FL, Renga G, Pariano M, Bellet MM, Servillo G, Fallarino F, et al. Anakinra restores cellular proteostasis by coupling mitochondrial redox balance to autophagy. *J Clin Invest* 2022;132:2.
50. van den Akker GGH, Steijns J, Stassen R, Wasilewski GB, Peeters LCW, Wijnands KAP, et al. Development of a cyclic-inverso AHSG/Fetuin A-based peptide for inhibition of calcification in osteoarthritis. *Osteoarthr Cartil* 2023;31(6):727–40.